AFRL-RZ-WP-TP-2010-2218

DYNAMIC TESTING OF ELECTROMECHANICAL ACTUATORS USING TIME-HISTORY DATA (PREPRINT)

Nicholas Rolinski

University of Dayton Research Institute

Quinn Leland, Earl Gregory, and Brett Jordan

Mechanical Energy Conversion Branch
Energy/Power/Thermal Division

David Woodburn and Thomas Wu

University of Central Florida

NOVEMBER 2010

AIR FORCE RESEARCH LABORATORY
PROPULSION DIRECTORATE
WRIGHT-PATTERSON AIR FORCE BASE, OH 45433-7251
AIR FORCE MATERIEL COMMAND
UNITED STATES AIR FORCE

REPORT DOCUMENTATION PAGE	Form Approved OMB No. 0704-0188

1. REPORT DATE *(DD-MM-YYYY)*	2. REPORT TYPE	3. DATES COVERED *(From - To)*
November 2010	Conference Paper Preprint	21 Feb 2009 – 02 Nov 2010

4. TITLE AND SUBTITLE
DYNAMIC TESTING OF ELECTROMECHANICAL ACTUATORS USING TIME-HISTORY DATA (PREPRINT)

5a. CONTRACT NUMBER In-House
5b. GRANT NUMBER
5c. PROGRAM ELEMENT NUMBER 62203F

6. AUTHOR(S)
Nicholas Rolinski (University of Dayton Research Institute)
Quinn Leland, Earl Gregory, and Brett Jordan (AFRL/RZPG)
David Woodburn and Thomas Wu (University of Central Florida)

5d. PROJECT NUMBER 3145
5e. TASK NUMBER 13
5f. WORK UNIT NUMBER 31451313

7. PERFORMING ORGANIZATION NAME(S) AND ADDRESS(ES)

University of Dayton Research Institute
300 College Park
Dayton, OH 45469

Mechanical Energy Conversion Branch (AFRL/RZPG)
Energy/Power/Thermal Division
Air Force Research Laboratory, Propulsion Directorate
Wright-Patterson Air Force Base, OH 45433-7251
Air Force Materiel Command, United States Air Force

University of Central Florida
4000 Central Florida Boulevard
Orlando, FL 32816

8. PERFORMING ORGANIZATION REPORT

9. SPONSORING / MONITORING AGENCY NAME(S) AND ADDRESS(ES)

Air Force Research Laboratory
Propulsion Directorate
Wright-Patterson Air Force Base, OH 45433-7251
Air Force Materiel Command
United States Air Force

10. SPONSOR/MONITOR'S ACRONYM(S)
AFRL/RZPG

11. SPONSOR/MONITOR'S REPORT NUMBER(S)
AFRL-RZ-WP-TP-2010-2218

12. DISTRIBUTION / AVAILABILITY STATEMENT
Approved for public release; distribution unlimited.

13. SUPPLEMENTARY NOTES
Conference paper presented at the Power Systems Conference, November 2010, in Fort Worth, TX. This paper contains color. PA Case Number: 88ABW-2010-5443; Clearance Date: 07 Oct 2010. The U.S. Government is joint author of the work and has the right to use, modify, reproduce, release, perform, display, or disclose the work.

14. ABSTRACT
A commercial electromechanical actuator (EMA) is to be dynamically tested with predetermined stroke and load profiles for transient thermal and electric power behavior to validate a numerical model used for aerospace applications. The EMA will follow the stroke profile representative of a real aircraft mission duty cycle. A hydraulic press will exert acorresponding load profile onto the EMA. Specialized hydraulic load control methods must be employed to meet the accuracy requirements. Two of these methods are closed-loop linearization (CLL) and displacement induced disturbance cancellation (DIDC). These methods are implemented along with an external PID compensator, and run in real-time in a series of system identification experiments to observe controller performance.

15. SUBJECT TERMS:
electromechanical actuator (EMA), transient thermal power, numerical model, aerospace, hydraulic press, closed-loop linearization (CLL), displacement induced disturbance cancellation (DIDC), more electric aircraft

16. SECURITY CLASSIFICATION OF:			17. LIMITATION OF ABSTRACT	18. NUMBER OF PAGES	19a. NAME OF RESPONSIBLE PERSON
					Quinn Leland
a. REPORT	b. ABSTRACT	c. THIS PAGE			19b. TELEPHONE NUMBER *(include area code)*
Unclassified	Unclassified	Unclassified	SAR	16	937-255-3060

10PSC-0085

Dynamic Testing of Electromechanical Actuators Using Time-history Data

Nicholas Rolinski
University of Dayton

Quinn Leland, Earl Gregory, Brett Jordan
Air Force Research Laboratory

David Woodburn, Thomas Wu
University of Central Florida

ABSTRACT

A commercial electromechanical actuator (EMA) is to be dynamically tested with predetermined stroke and load profiles for transient thermal and electric power behavior to validate a numerical model used for aerospace applications. The EMA will follow the stroke profile representative of a real aircraft mission duty cycle. A hydraulic press will exert a corresponding load profile onto the EMA. Specialized hydraulic load control methods must be employed to meet the accuracy requirements. Two of these methods are closed-loop linearization (CLL) and displacement induced disturbance cancellation (DIDC). These methods are implemented along with an external PID compensator, and run in real-time in a series of system identification experiments to observe controller performance.

INTRODUCTION

Electromechanical actuators (EMA) may offer significant benefits over their hydraulic counterparts for some aerospace applications as viable designs stem from the industry-wide more-electric-aircraft trend. EMA thermal and electric power behavior must be examined and managed for successful technology emergence to occur. In the process of examining these behaviors, physical observation through testing must take place. Test output data can be used for a host of purposes including hardware-in-the-loop experimentation, model validation, prognostics studies, and more. For this study, the physical experimentation serves as a method for thermal and electric power, transient-model validation. For this test, a Danaher EMA (EC-5) and an MTS hydraulic press (MTS 458.20 controller) are used. The EMA is commanded to follow a stroke profile representative of a real aircraft mission duty cycle. The hydraulic press is commanded to exert a corresponding load profile. Due to the limitation of the selected hardware and flight environment for the actuator, physical testing can become a complex task involving time-history data streaming, test component synchronization, profile parameter scaling, and specialized closed-loop control techniques. The latter of these topics is examined here. In considering possible specialized closed-loop control techniques for implementation, two primary sources of error are significant. They are the load disturbance related to EMA stroke rate, or velocity (called displacement-induced load disturbance) and the mathematical result of an undesired PID compensator embedded in the press control hardware. They are shown in Figure 1, which shows the hydraulic press control loop. A proposed mitigation of the first error source is called displacement induced disturbance cancellation, or DIDC. For the second error source, a proposed mitigation method is called closed-loop linearization, or CLL. These respective solutions are investigated, implemented and validated through physical testing.

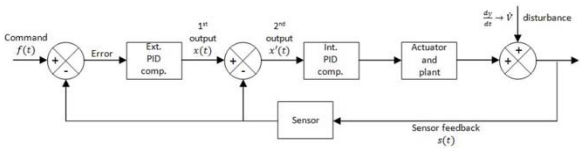

Figure 1. Hydraulic press closed-loop control with two specialized problems related to EMA testing: displacement-induced load disturbance, and the presence of an undesired PID compensator. The input signal $f(t)$ is the load command.

DESIGN OF A HARDWARE-BASED EXPERIMENT USING A REAL MISSION PROFILE

To ensure that the model is applicable to aerospace actuation designs, an emulated flight environment is selected for hardware testing. This is made possible using recorded actuator load and stroke data from a real mission profile captured during a test flight onboard the NASA F-18 Systems Research Aircraft [1]. Under the assumption that there is no appreciable relationship between load and stroke that can be closely replicated,[1] the data is treated as if specific, independent load and stroke values exist for each time step. Experimentally, the EMA is commanded to execute the stroke profile recorded during the actual flight so that the effect of a pilot performing flight maneuvers is achieved in the exact order as observed during the real flight. Meanwhile, the corresponding recorded loads must be exerted on the test article by an external source in order to replicate the flight specific duty cycle in terms of mechanical power outputs of the motor and controller. In this case, a hydraulic actuator controlled with a current-driven servo valve is selected. The flight emulation components of the test make it a unique application of hydraulics, since the test article drives stroke, rather than simply providing a passive load. The full assembly is fixed in a high-load frame, shown in Figure 2.

[1] Load and stroke relationships have been established for given control surfaces and flight profiles. For one example, please see *Kang, Pachter, Houpis.*[2]. For the case of the hydraulic press and controller used for this effort, such methods were found to be more difficult to use for physical load environment emulation.

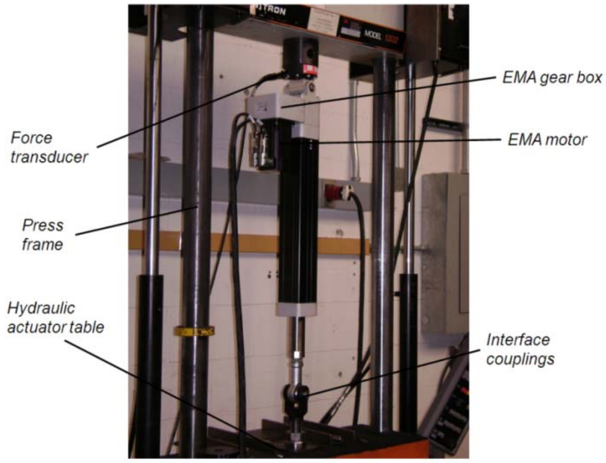

Figure 2. Hydraulic press arrangement where the EMA is subjected to conditions consistent with what is observed in real flight.

The process of model validation requires the model simulation to be executed first to determine the appropriate locations for physical instrumentation, such as thermocouples and electrical sensors. The model identifies these locations by capturing temperature maxima referred to as "hotspots", which in turn provide the test engineer rationale for instrumenting the hardware at certain nodes of interest within the actuator hardware. Instrumentation is most often installed in the actuator motor and motor controller. Once properly instrumented, the hardware can be tested for thermal and electric power behavior, and the results can be used for model checking.

HYDRAULIC PRESS CONTROL

The hydraulic press controller employs a common hardware embedded closed-loop PID compensator in order to accurately control either load or position exclusively. It is referred to as the internal PID compensator. When in load control mode, the press controller can closely control the load exerted on the EMA but cannot control the position of the hydraulic actuator head. Stroke control mode allows the press controller to closely control the stroke of the hydraulic actuator head without regard to the loading which may result. On the press controller, the proportional, integral and derivative gain values are open to user tuning. While this arrangement is common for many devices, difficulty arises for load control when the EMA moves abruptly as called for in this unique test. This stems from the inherent relationship between pressure and volume for hydraulic systems where the fluid is considered incompressible, and where volume is changed by external input from the EMA. If the EMA delivers a tensile force by retracting, suction is created locally inside the hydraulic actuator, resulting in a decreasing deviation from the commanded load. In contrast, if the EMA delivers a compressive force by extending, the volume decreases causing the pressure and load to increase. In the case of compression, the incompressibility of the hydraulic fluid causes the fluid to be evacuated from the actuator cylinder leading to added flow work thus causing the load increase rather than fluid compression. While a set of tuned PID values allows for accurate control of load, the classically designed internal PID compensator does not accommodate for abrupt EMA displacement associated with the execution of a stroke profile. However, by taking advantage of the relationship between hydraulic actuator pressure, or load and volume, a link is established between the two parameters and the displacement can therefore be addressed as a load disturbance. The EMA velocity corresponds to a volumetric rate of change of the hydraulic actuator since they are rigidly coupled. Figure 3 shows how the displacement induced disturbance influences the true load, or the sensor feedback signal $s(t)$. Note that displacement is only relevant on a time rate of change basis, where the EMA is in motion. Therefore the disturbance is expressed as a velocity in the block diagram.

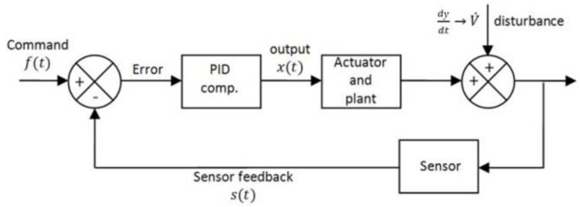

Figure 3. Displacement induced disturbance in load. Here, the plant model is treated as an unknown.

By viewing the figure, it can be inferred that high speed EMA motion severely degrades pressure consistency and controllability. By obtaining the EMA velocity at every loop execution, multiplying it by a tunable gain value, and adding the result to the PID error compensation, the error component due to displacement is nullified. This technique is also referred to in this paper as displacement induced disturbance cancellation, or DIDC. In order to implement DIDC, an in-house closed-loop compensator must be designed and built external to the provided hardware, since the internal PID compensator is limited to classical single parameter control (proportional, integral and derivative gains). The additional compensator must have standard PID features as well as specialized components such that no control capability is lost in replacing the internal PID compensator. The compensator equation is expressed as:

$$x(t) = k_p\big(f(t) - s(t)\big) + k_i \int \big(f(t) - s(t)\big)\, dt + k_d \frac{d}{dt}\big(f(t) - s(t)\big) + k_y \frac{dy}{dt} \qquad (1)$$

where $f(t)$, $x(t)$, and $s(t)$ represent load command, compensator output, and sensor feedback, respectively, as indicated in Figure 3, and k_p, k_i and k_d represent standard proportional, integral and derivative gains, respectively. Note that the final term in eq. (1) operates on a different independent variable than error, called y. This variable is stroke, and its time rate of change is the EMA velocity. It includes a tunable gain multiplier called k_y. The PID gains are tuned with k_y for proper DIDC implementation.

One alternative to using the DIDC, is to use a “learning” algorithm, which is an iterative process where the original time-history data is executed by the system with little to no closed-loop tuning (some limit interlocks may be necessary for safety). Upon receiving the feedback profile, the error incurred is used to manipulate the original time-history profile. This is done until an empirical transfer function is embedded into the input time-history profile such that the plant produces the originally desired input profile due to its inherent error contribution. The team chose not to use such a method since it cannot be adapted to an input profile generated in real-time. Although running real-time generated profiles is not a current application, it is desirable to have such capability in the future.

Additionally, the internal PID compensator must be deactivated or bypassed in order to maintain linearity, since the two compensators would otherwise be configured in series, which would cause undesired algebraic effects, as shown later. The internal PID compensator allows integral and derivative gain values to be tuned to zero, but the proportional gain value may never be tuned to less than one. In other words, it can never be fully removed by tuning alone. Therefore, the external PID compensator must include an additional operation to cancel out the internal PID compensator's effect. Figure 4 illustrates the compensators in series.

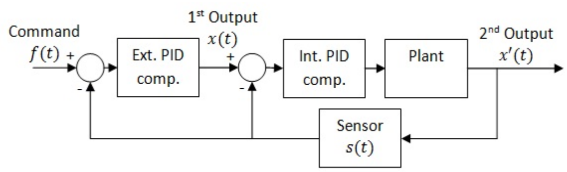

Figure 4. In-series PID compensator arrangement with an external PID compensator built to include DIDC.

The block diagram in Figure 4 can be expressed algebraically by

$$x'(t) = P\left[k_{p2}(x(t) - s(t))\right] \quad (2)$$

where P represents a model of the plant, k_{p2} represents the proportional gain value for the internal PID compensator and $x(t)$ equals the output of the external PID compensator. More specifically, $x(t)$ is defined by:

$$x(t) = k_{p1}(f(t) - s(t)) \quad (3)$$

where k_{p1}represents the proportional gain value for the external PID compensator. Substituting the RHS of eq. (3) into eq. (2) gives:

$$x'(t) = P\left\{k_{p2}\left[k_{p1}(f(t) - s(t)) - s(t)\right]\right\} \qquad (4)$$

Notice that only proportional gain compensation is included in (3), for the full expression for the external PID compensator, integral, derivative and DIDC terms may be included. They are omitted here for simplicity. The effect of the internal PID compensator and the requirements for its cancellation per Figure 4 are shown as follows. First, notice that the external PID compensator uses error for its input, calculated by:

$$Error = f(t) - s(t) \quad (5)$$

This is a comparison of two load signals, $f(t)$ and $s(t)$. For a proper comparison, both signals must be of the same nature. In the case of (2
), the two load signals are scalar quantities expressed as either volts or load units. Both signals (command and sensor feedback) are free of conditioning and correction. For the internal PID compensator, the comparison is inappropriate, since its error is calculated by:

$$Error = x(t) - s(t) \quad (6)$$

where $x(t)$ is a signal that has already been corrected, and is used as the intended output to the plant. Therefore, cancellation of the internal PID compensator is necessary. Figure 5 shows how the block diagram can be modified to provide this cancellation. The sensor signal is simply added to the signal $x(t)$, so that the result of the local (second) summation is not another comparative error, but rather the input to that junction (no change takes place). In LabVIEW, it is easy to add the sensor signal $s(t)$ to the output $x(t)$.

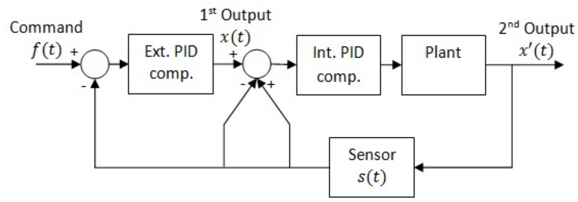

Figure 5. Block diagram for cancellation of internal PID compensator. Notice that the sensor signal $s(t)$ is subtracted and added in the second summing junction, resulting in no summation effect.

Now, the external PID compensator and the internal PID compensator are simply two blocks in series, but the external PID compensator block offers a simple contribution, it is now a factor of k_{p2} multiplied on the input. Manually tuning this gain value to 1 is equivalent to removing it, as shown in Figure 6.

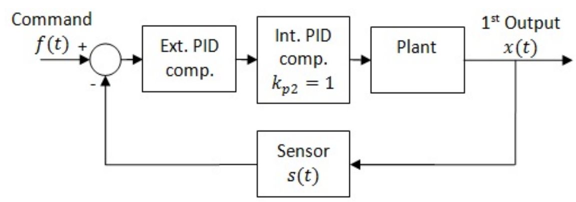

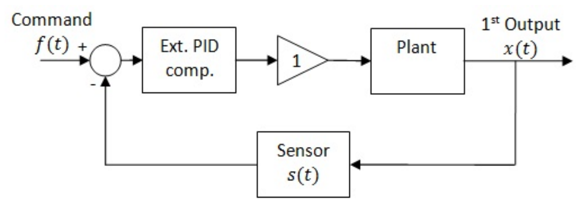

Figure 6. Compensator and plant arrangement with full cancellation. After the sensor signal is cancelled out as shown in Figure 5, the gain value k_{p2} is tuned to 1 (top block diagram) which produces the classical control loop shown by the bottom block diagram.

Notice the cancellation of the sensor signal $s(t)$:

$$x'(t) = P\{k_{p2}[k_{p1}(f(t) - s(t)) - s(t) + s(t)]\} = P[k_{p1}(f(t) - s(t))] \quad (7)$$

Therefore, (7) shows how the desired signal is modified by the internal PID compensator. To cancel out these effects, modifications must be made in the algorithm where the signal becomes $x(t)$ (the point at which the signal is passed from the external PID compensator to the internal PID compensator). It is shown in eq. (7) that the signal is altered as a result of the internal PID compensator in two ways: the sensor magnitude $s(t)$ is subtracted and the internal PID controller gains are multiplied on the signal. Therefore, by ensuring that the sensor signal is added, to cancel out the subtraction of the same signal, and that the proportional gain k_{p2} is set equal to 1, the internal PID compensator is cancelled out, allowing for clean and predictable PID control. The final compensator equation features CLL and DIDC and is expressed as follows:

$$x(t) = k_p\big(f(t) - s(t)\big) + k_i \int \big(f(t) - s(t)\,\big)dt + k_d \frac{d}{dt}\big(f(t) - s(t)\big) + k_y \frac{dy}{dt} + s(t) \quad (8)$$

A non-displacement test is carried out to try the new external PID compensator and to tune the PID gain values. Such a procedure is completed by installing a rigid member into the hydraulic press and controlling load. A square wave is used since it contains a wide range of frequencies and, therefore, helps to reveal the frequency response of the system. Figure 7 shows the test results which match previously recorded results of the internal PID compensator under similar testing conditions. The Ziegler-Nichols [3] tuning heuristic is loosely followed to locate an optimized gain set for the PID control. This method is used in the absence of knowing what the plant transfer function is. As the plot indicates, the steady-state error is very low while the transient error is very high. Transient error may be reduced by adding a feed-forward component to the external PID compensator in the future, since time-history data is known for all times prior to being executed. Nevertheless, the test results indicate the effectiveness of the CLL method.

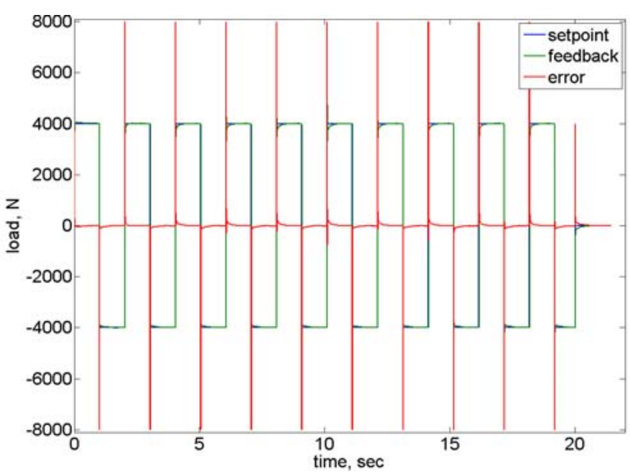

Figure 7. Press load performance using in-house built external PID compensator. The internal PID compensator is still present but nullified.

After tuning gain values, the proceeding step is to install the EMA to execute a stroke profile where both specialized methods, CLL and DIDC, are employed. Preliminary results for utilization of both methods appear to indicate moderate success in CLL and DIDC. However refined tuning is still required. Results have been obtained per operator visualization during test operation. However, logged test data was destroyed by a hydraulic line failure during the test. Future work includes gathering data of this kind, tuning and adding additional higher-order terms and feed forward to (8) to improve the control performance.

CONCLUSION

To ensure applicability to the aerospace industry, it is beneficial to use real flight data in physically emulating the load environment for EMA model validation. Specialized control methods must be implemented to accommodate for the inherent traits of the real mission profile. Since real data is called from time-history read tables, load and stroke control operate on the press and EMA, respectively, completely independent of each other, but linked by the time stamp. Another link arises between the two data sets from the existence of the relationship between the pressure and volume flow of the press's hydraulic system, and thus load and velocity. This paper attempts to describe these preliminary findings and offer simple but effective methods for control which can be used in lab setup testing and initial data gathering. One specialized method called displacement induced disturbance cancellation, or DIDC, has been closely examined, tested, and validated per limited visual inspection during testing. A second specialized method called closed-loop linearization, or CLL, has been used to cancel the influence of an undesired PID controller within the main control loop: a commonly encountered problem associated with commercially available hardware used for specialized testing applications. Future work includes optimization and further development of the DIDC method and addition of higher-order terms and a feed forward term to the compensator to improve performance. Additionally, use of time-history data for higher-order compensation (e.g. use time-history velocity and acceleration rather than on-the-fly sampled and calculated velocity and acceleration) should be explored. Finally, it is concluded that building external closed-loop compensators requires careful consideration of the requirements to maintain system linearity and consistency. This step is necessary anytime a custom fix such as DIDC is added to classical closed-loop PID compensator design.

REFERENCES

[1] Jensen, Stephen C., Gavin D. Jenney, Bruce Raymond, and David Dawson. *Flight Test Experience with an Electromechanical Actuator on the F-18 Systems Research Aircraft*. 19th Digital Avionics Conference proceedings. Volume 1. Pages 2E3/1-2E310. Printed 2000. ISBN 0-7803-6395-7.

[2] Kang, K., M. Pachter, C. H. Houpis, and S. Rasmussen. *Modeling and Control of an Electro-Hydrostatic Actuator*. International Journal of Robust & Nonlinear Control. Volume 7. Issue 6. Pages 591-608. 1998.

[3] Abramovici, Alex, and Jake Chapsky. *Feedback Control Systems: a Fast-track Guide for Scientists and Engineers*. Boston: Kluwer Academic, 2000.

CONTACT INFORMATION

Quinn Leland, Quinn.leland@wpafb.af.mil, Air Force Research Laboratory, Dayton, OH

ACKNOWLEDGMENTS

The authors wish to acknowledge the funding support provided by AFRL under contract FA8650-04-D-2403 (D013). Technical contributions were given by Jon Zumberge of AFRL, Dr. Tommy Baudendistel of PCKA and Jeffery Roach and James Sheehan of Boeing. The following people also provided valuable technical advice: Peter Lamm of AFRL, Laura Lyle of Taitech, and Steve Emo and Brian Harris of UDRI. Laboratory facilities and equipment have been provided by Joseph Weimer, Dr. Russell Spyker and Dr. Joseph Fellner of AFRL. Mission profile data was provided by Ben Tran and Will Stout of AFRL. Technician support was provided by Tom Greene of Taitech and Cameron Riepenhoff of UDRI. Academic advising was provided by Dr. Kevin Hallinan of the University of Dayton and Dr. Louis Chow of the University of Central Florida.